

Formation of the Newly Greenish Organized Molecular Film of Long-Chain Diynoic Acid Derivatives by Photopolymerization and Its Structural Study Using Near-Edge X-ray Absorption Fine Structure (NEXAFS) Spectroscopy

Atsuhiko Fujimori,^{*,#} Mikako Ishitsuka, and Hiroo Nakahara

Department of Chemistry, Faculty of Science, Saitama University,
Shimo-okubo, 255, Sakura-ku, Saitama 338-8570, Japan

Eisuke Ito and Masahiko Hara

Local Spatio-Temporal Function, Frontier Research System, The Institute of Physical and Chemical Research (RIKEN), Hirosawa 2-1, Wako 351-0198, Japan

Kaname Kanai,[†] Yukio Ouchi,[†] and Kazuhiko Seki^{†,‡}

Department of Chemistry, Graduate School of Science, Nagoya University, and Research Center for Materials Science, Nagoya University, Furo-cho, Chikusa-ku, Nagoya 464-8602, Japan

Received: January 30, 2004; In Final Form: June 22, 2004

The effect of molecular arrangements with annealing on photopolymerization in the Langmuir–Blodgett films of 10,12-pentacosadiynoic acid cadmium salt was investigated using UV–vis spectroscopy, out-of plane and in-plane X-ray diffraction (XRD), and polarized near-edge X-ray absorption fine structure (NEXAFS) spectroscopy. The formation of a greenish polymer film with an extended conjugate system was determined to be related to the film structures. Furthermore, the incident-angle dependence of C1s– π^* transition peaks on the annealed transferred film with an extended conjugate system was confirmed by C K-edge polarized NEXAFS spectroscopy, whereas this dependency was not observed on nonannealed multilayer films. In addition, multilayers of metal-free 10,12-pentacosadiynoic acid were examined by photopolymerization, and their film structures were elucidated. Contrary to expectations, a red-colored polymer film was observed to form highly ordered side-chain orientations with the shift of the C1s– π^* transition peaks in the NEXAFS spectra, although the regularity of molecular and side-chain arrangement for monomer and blue polymer films could not be confirmed. These findings indicate the color phase transition of diacetylene derivatives with photopolymerization induced the rearrangement of the conjugated backbone, supported by a shift of the C1s– π^* band in the NEXAFS spectra.

1. Introduction

Many types of diacetylene derivatives ($R-C\equiv C-C\equiv C-R'$) polymerize under UV irradiation, forming blue- or red-colored polymers with conjugated π -electron systems. This polymerization reaction proceeds in various states such as single crystals,¹ Langmuir–Blodgett (LB) films,² self-assembled monolayers,³ and evaporated films.⁴ The interest in diacetylene polymers has been accelerated by a recent proposal of their use as nonlinear optical and electro-optical devices.^{5,6} Approximately thirty years ago, Wegner et al.¹ reported that diacetylene derivatives form a wide variety of polymer architectures, ranging from thick and thin films to crystals, bilayers, and monomolecular layers.^{3,7–12} It was later reported that the polymerization of amphiphilic monomers such as long-chain vinyl esters and long-chain diynoic acid significantly progressed and the structure of the resulting polymers could be controlled in LB films.^{13,14} In

addition, UV photoelectron spectroscopy (UPS) and preliminary C K-edge near-edge X-ray absorption fine structure (NEXAFS)^{15,16} studies through UV photopolymerization in 10,12-tricosadiynoic acid cadmium salt LB films were compared with those for the acid-free form of the evaporated films.^{17–21} The color phase transition of polydiacetylene was initially ascribed to the two possible resonance structures: acetylenic and butatrienic. However, it was later suggested, based on the results of UPS measurements, that both the blue and red polymers formed the acetylenic structures.^{18,20} A slight fluctuation the hydrocarbon side-chain packing is currently considered to be the cause of these color phase transitions with UV irradiation, thermal treatment, or exposure to organic solvents, although the change in the detailed electronic state is not clear. Recently, the diacetylene monomer-to-polymer conversion efficiencies in the films were measured by fluorescence yield near-edge spectroscopy (FYNES) in the C1s– π^* region (280–286 eV).²²

In the present study, the monolayer behavior on the water surface, and the effect of molecular arrangements with annealing on photopolymerization in cadmium 10,12-alkyldiynoate LB films are investigated by surface pressure–area (π –A) isotherms, UV–vis spectroscopy, X-ray diffraction (XRD), and in-plane XRD. In addition, the formation of a novel greenish

* Author to whom correspondence should be addressed: Telephone: +81-238-26-3073. Fax: +81-238-26-3073. E-mail: fujimori@yz.yamagata-u.ac.jp.

Present address: Department of Polymer Science and Engineering, Faculty of Engineering, Yamagata University, Jonan 4-3-16, Yonezawa, Yamagata, 992-8510 Japan.

[†] Department of Chemistry.

[‡] Research Center for Materials Science.

polymer film from cadmium salt with an extended conjugate system was determined to be related to the film structures. The molecular orientation and alignment of functional groups were estimated by polarized NEXAFS spectroscopy. Furthermore, the process of photopolymerization and the change of the NEXAFS spectra for the transferred film of metal-free 10,12-alkyldiynoic acid are compared with that of its cadmium salt, and the origin of the color phase transition for polydiacetylene is discussed.

2. Experimental Section

10,12-Pentacosadiynoic acid (DA[11–8], $\text{CH}_3(\text{CH}_2)_{11}-\text{C}\equiv\text{C}-\text{C}\equiv\text{C}-(\text{CH}_2)_8\text{COOH}$) was obtained from Dojin Chemical Laboratories and purified via four-times recrystallization from a chloroform:*n*-hexane (1:9, v/v) mixed solvent. These monolayers were spread onto the distilled water (above 18.2 MΩ cm, pH 5.8) and an aqueous subphase containing 3×10^{-4} M CdCl_2 and 5×10^{-4} M KHCO_3 (pH 6.8). The surface pressure–area (π –*A*) isotherms for the monolayers were measured using a Lauda film balance at 15 °C. The multilayers were deposited at 25 mN/m and a temperature of 15 °C as a cadmium salt (cadmium 10,12-pentacosadiynoate, abbreviated as CdDA[11–8]) by the Langmuir–Blodgett (LB, vertical dipping) method²³ and transferred by the horizontal lifting method²⁴ at 11 mN/m and a temperature of 15 °C as metal-free acid films, because of the lower collapsed surface pressure at ~ 16 mN/m for DA[11–8] monolayers (typically up to 20 layers) onto the solid substrate coated with three layers of cadmium stearate or an iron stearate monolayer (XRD measurements) to achieve a hydrophobic surface.^{25,26} The annealing conditions for the cadmium-salt transferred films were examined in the range of 45–65 °C (± 1.0 °C) and reacted for 1–120 h in a thermostated water tank to form the highly developed molecular arrangement. As a result of this experiment, the highest oriented molecular alignment was observed to form at 50 °C after 72 h, as estimated by XRD measurements before and after annealing of the monomer multilayered films. Photopolymerization was conducted by exposing the films to a 500 W xenon lamp at a distance of 40 cm. The dependence of the extent of polymerization on the irradiation time was examined by measuring the absorption spectra (using a Hitachi model U-3210 spectrometer) of the transferred films on a quartz plate. The values of the long spacing for the layered structures of the deposited films were measured using an X-ray diffractometer (Rigaku, Rad-B, Cu K α radiation, 40 kV, 30 mA) equipped with a graphite monochromator. The in-plane spacing of the two-dimensional lattice of the films was determined by analysis with an X-ray diffractometer with different geometrical arrangements²⁷ (Bruker AXS, MXP-BX, Cu K α radiation, 40 kV, 40 mA) equipped with a parabolic graded multilayer mirror. NEXAFS spectra were measured on BL-7A soft X-ray beamlines at the Photon Factory in the National Laboratory for High-Energy Accelerator Research Organization (KEK–PF) with synchrotron radiation from a bending-magnet source.^{28,29} The C K-edge spectra were measured in the photon energy region of 275–325 eV, and in partial electron yield mode (PEY)^{15,30} with a retarding voltage of -200 V under a vacuum of 10^{-8} Torr. In the NEXAFS measurements, monolayers were transferred onto a conducting tin oxide coated glass substrate (NESA) with the hydrophobic treatment.

3. Results and Discussion

Photopolymerization in the Transferred Films and Formation of the Greenish Polymer Film for CdDA[11–8]. In the π –*A* isotherm of the CdDA[11–8] monolayers at 15 °C,

DA[11–8] formed a stable condensed monolayer as a cadmium salt on the aqueous subphase containing CdCl_2 and KHCO_3 (pH 6.8), with a limiting molecular area of 22.5 \AA^2 . Based on our preliminary experiment, amphiphilic DAs contain longer hydrocarbon tails, as well as 10,12-heptacosadiynoic acid (DA[13–8]) and nonacosadiynoic acid (DA[15–8]) diynoic acids with limiting molecular areas of 27.0 and 30.2 \AA^2 , respectively. These findings were in good agreement with the results of a previous study on diacetylene that were reported by Teike et al.³¹

Photopolymerization of CdDA[11–8] molecules in multilayers prepared by LB methods (20 layers, 25 mN/m, 15 °C), in addition to the effect of annealing, was investigated. The packing mode of the monomer molecules and the size of the domain in monolayer assemblies have a significant influence on the polymerization reaction and the structure of the resultant polymers. As shown in Figure 1, CdDA[11–8] polymers formed rapidly upon irradiation with UV light. In the nonannealed LB film (Figure 1A), the rapidly polymerized blue polymer exhibited an absorption maximum at 638 nm in UV–vis spectra by UV irradiation and the spectra changed readily from blue to red, while annealed LB multilayers (50 °C, 72 h) were the most suitable conditions to form highly ordered molecular orientations; see Figure 1B) polymerized very rapidly and became green, with a maximum absorption wavelength of $\lambda_{\text{max}} = 705$ nm. On the other hand, untreated LB films had a maximum wavelength of $\lambda_{\text{max}} = 638$ nm in blue films. The band shift to a longer wavelength was considered to be primarily due to the contribution of the highly extended π -conjugate system, based on a simple free-electron model.³² In addition, the greenish film changed to blue and finally to red after extended exposure to UV irradiation. The formation of this greenish polymer film, which had an extended conjugate system, by annealing and UV irradiated photopolymerization were confirmed on the CdDA[11–8] LB film. On the other hand, CdDA[13–8] and CdDA[15–8] exhibited rather irregular surface structures and could not form the greenish films under any annealing conditions. The greenish polymer backbone not only had an extended conjugate system but also may exhibit a higher degree of polymerization and larger domain size in the surface, compared to the blue nonannealed monomer film.

Figures 2 and 3 show the difference between the out-of-plane and in-plane XRD profiles of annealed and nonannealed CdDA[11–8] multilayers with UV photopolymerization. From these results, development of layer structure and packing of the hydrophobic chains in the plane (subcell structure) were clearly indicated. Figure 2A shows the first-order diffraction peaks for several films in annealed and nonannealed multilayers. These results revealed that CdDA[11–8] molecules in the LB films developed layered structures and the growth of the structures was enhanced when they were annealed, supported by an increase of the peak intensity for the XRD profiles (Table 1). The tilt angle of the CdDA[11–8] molecules in the films was $\sim 41^\circ$. In addition, the higher-order diffraction peaks are shown in Figures 2B and 2C. The appearance of higher-order diffraction peaks was confirmed to be due to the development of the layered structures formed in LB films on annealing. Furthermore, the change in the two-dimensional lattice was observed to be almost the same on both annealing and polymerization (see Figure 3). That is, the monomer film formed hexagonal subcells^{30,33} with short spacing ($d = 4.47 \text{ \AA}$); however, the blue polymer and annealed films typically formed triclinic subcell systems, because of their tilted molecular orientation and distorted in-plane lattices. However, short spacing peaks for red polymers were not confirmed in both systems. The effect of preannealing

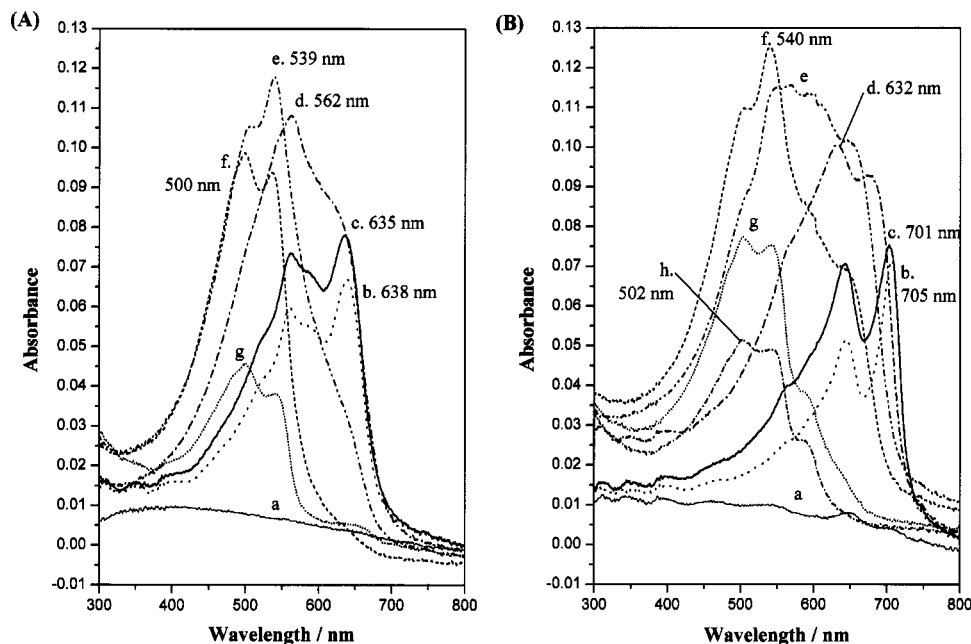


Figure 1. Change of visible absorption spectra of cadmium salts of DA[11–8] through photopolymerization in Langmuir–Blodgett films (20 layers deposited at 25 mN/m, 15 °C): (A) nonannealed and (B) preannealed at 50 °C for 72 h, with UV-irradiation periods of 0 min (spectrum a), 1 min (spectrum b), 2 min (spectrum c), 10 min (spectrum d), 20 min (spectrum e), 30 min (spectrum f), 1.0 h (spectrum g), and 1.25 h (spectrum h).

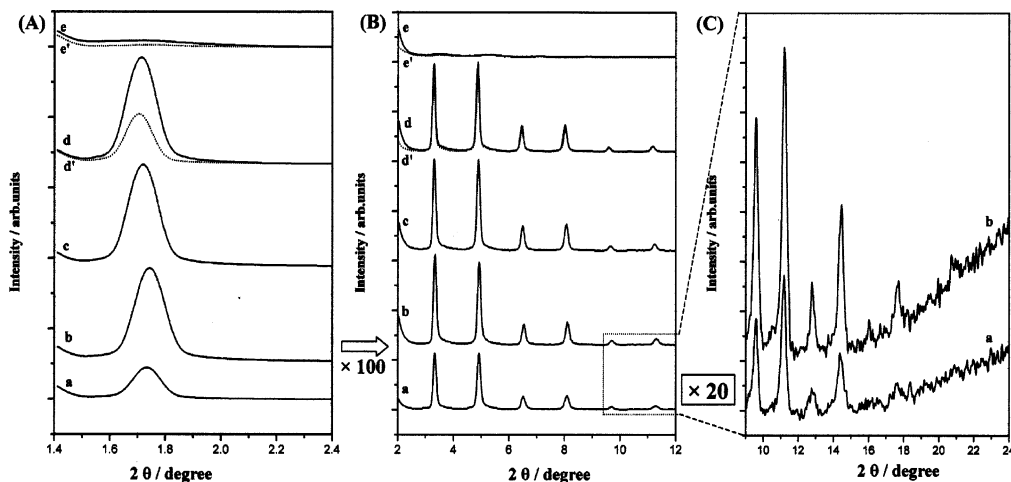


Figure 2. Change of out-of plane XRD profiles in different extended axis scales: (A) small-angle region, (B) $2\theta = 2^\circ\text{--}12^\circ$, and (C) wide-angle region for cadmium salts of DA[11–8] LB films (20 layers deposited at 25 mN/m, 15 °C) through the photopolymerization ((nonannealed (spectrum a), annealed monomers at 50 °C for 72 h (spectrum b), green Poly-CdDA (spectrum c), blue Poly-CdDA (spectrum d), and red Poly-CdDA (spectrum e) (dotted lines labeled d' and e' were obtained from the nonannealed CdDA monomer LB film).

involved the formation of a two-dimensional lattice structure, which resulted in the effective polymerization. These structural phase transitions, from isotropic hexagonal to the triclinic subcells, indicate that in-plane anisotropy is related to the polymerization process.

Near-Edge X-ray Absorption Fine Structure (NEXAFS) Spectroscopic Study for the CdDA[11–8] Transferred Films.

Figure 4 shows the curve-fitting analysis of the C K-edge NEXAFS spectra for CdDA[11–8] annealed multilayers with both normal and grazing X-ray incidence. The transition bands from the C1s level were assigned as listed in the table below Figure 4. The NEXAFS spectra at the C K-edge of the CdDA[11–8] films were fitted by several Gaussian functions, from low to high photon energy, and each band was assigned according to literature values.^{34–39} The peak in the lower-energy region was assigned to the transition from the C1s level to π^* -(C=C), which was believed to contribute to the orientation of

functional groups. Peaks “b” and “d” in Figure 4 were assigned to transitions from the C1s level to the σ^* (C–H) and σ^* (C–C) levels, respectively. These transitions primarily contributed to the molecular orientation along the long molecular axis.

Figures 5 and 6 show the dependence of the incident angle on the C K-edge NEXAFS spectra of the LB multilayers of CdDA[11–8], mainly to examine the orientation and electronic state of the conjugated backbone. Panels A, B, and C in Figure 5 respectively correspond to the NEXAFS spectra of the nonannealed CdDA[11–8] monomer film, the Poly-CdDA[11–8] blue film obtained by UV irradiation to the nonannealed CdDA[11–8] monomer film, and the Poly-CdDA[11–8] red film obtained by further UV irradiation. The spectra shown in Figure 5A were observed to be significantly dependent on the incident angle. The peaks at 287.6 and 290.7 eV were assigned to the transitions from the C1s level to the σ^* (C–H) and σ^* (C–C) orbitals, respectively. The relative

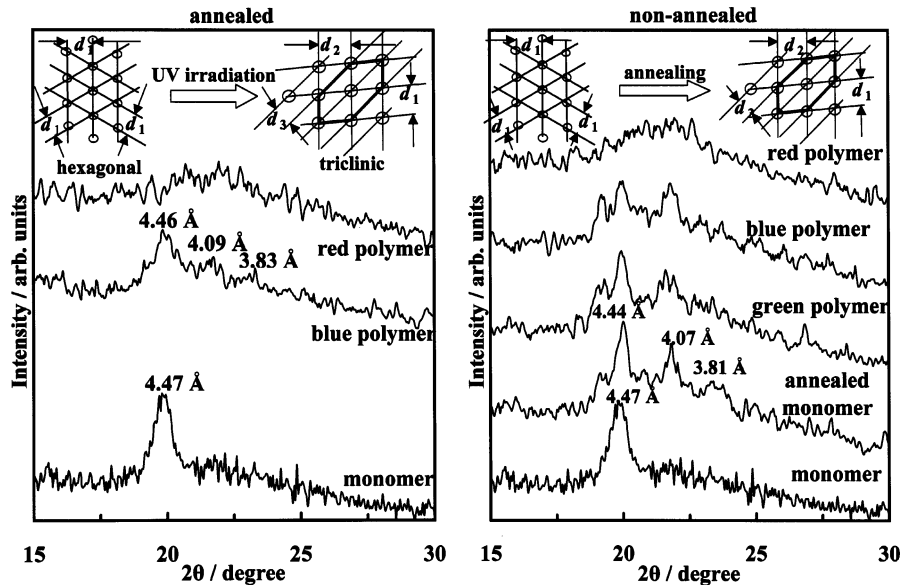


Figure 3. In-plane XRD profiles of nonannealed and annealed LB multilayers (20 layers, 25 mN/m, 15 °C) of CdDA[11-8] and their polymers on a glass substrate.

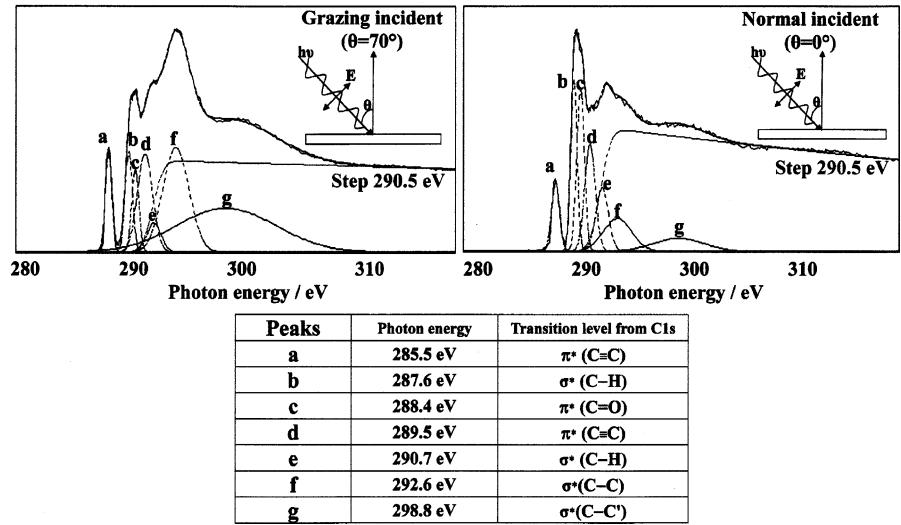


Figure 4. Curve fitting of the C K-edge NEXAFS spectra for the annealed CdDA[11-8] multilayers (20 layers, 25 mN/m, 15 °C). Their assignments are given in the table below the figure.

TABLE 1

	<i>d</i> (long spacing) (Å)		intensity (cps)	
	1st order	2nd order	1st order	2nd order
before annealing	55.5	28.1	78 340	1996
after annealing	54.1	27.5	104 688	2539

intensity of the $\sigma^*(\text{C-H})$ peak can be attributed to the C-H bonds in the hydrocarbon side chains. The $\sigma^*(\text{C-H})$ transition peak is maximum at normal incidence and is weakened at grazing incidence ($\theta = 70^\circ$). These results suggested that the transition moments of the 287.6 eV band were almost parallel to the surface, indicating an almost-perpendicular orientation of the hydrocarbons. However, the transition peaks from the C1s level to the $\pi^*(\text{C}\equiv\text{C})$ level were not observed to be dependent on the incident angle. This observation indicated the formation of a relatively random conformation or an inclination at the magic angle of the functional groups in the molecules. The results shown in Figure 5B reveal a slight polarization dependence at the C1s- π^* peak in the blue films after UV irradiation. The difference between Figure 5A and Figure 5B

was not remarkable, although it was supposed that the confirmation of stile incident angle dependence was based on rearrangement of the functional groups, together with the polymerization reaction. Thus, the lack of dependence on the incident angle for both the monomer and blue polymer films indicated the formation of a relatively random conformation, rather than an orientation to the magic angle. Both spectra showed an unclear polarization dependence for the C1s level to the π^* transition peaks, compared with the dependence on polarization for the C1s level to $\sigma^*(\text{C-H})$ and $\sigma^*(\text{C-C})$ transitions, which were responsible for the formation of the highly ordered molecular orientation of the molecules in LB films. The regularity of arrangement for the entire molecule arrangement along the long molecular axis and the functional groups were observed to decrease in the red films. In addition, NEXAFS spectra revealed that the red films were not dependent on the incident angle. The photon energy levels of the C1s-to- π^* transition along the lateral axis shifted from 285.5 eV to 285.0 eV. This energy shift is believed to be due to the difference in the π^* transition energy levels.

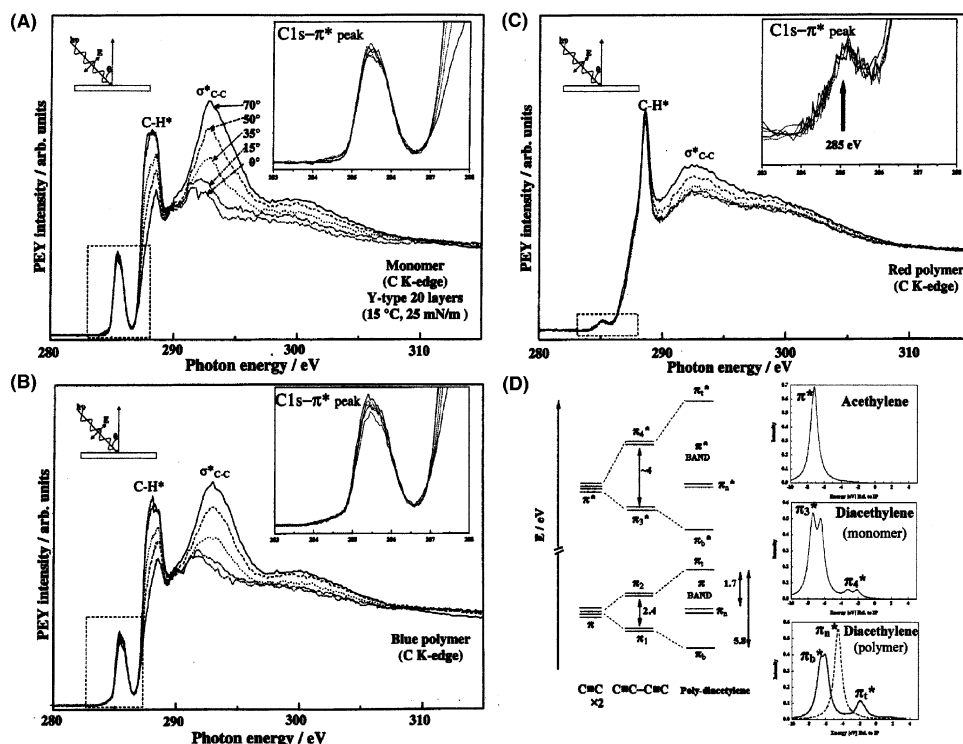


Figure 5. Dependence of the incident angles on the C K-edge polarized NEXAFS spectra for LB multilayers (20 layers, 25 mN/m, 15 °C) of CdDA[11–8] (A) monomer, (B) blue polymer, and (C) red polymer on NESA glass substrate. The right-hand side of panel d shows an energy-level diagram of acetylene, diacetylene, and polydiacetylene; the lower and upper halves correspond to the occupied and vacant states, respectively. The left-hand side of panel d shows simulated NEXAFS spectra by equivalent core MO calculations with CNDO/S method: (a) acetylene, (b) diacetylene, and (c) a model molecule of the diacetylene polymer $\text{CH}_2=\text{CH}-(\text{C}\equiv\text{C}-\text{C}=\text{C})_3-\text{H}$. In panel c, the solid and broken lines correspond to the electric vector of the light parallel and vertical to the molecular plane, respectively.

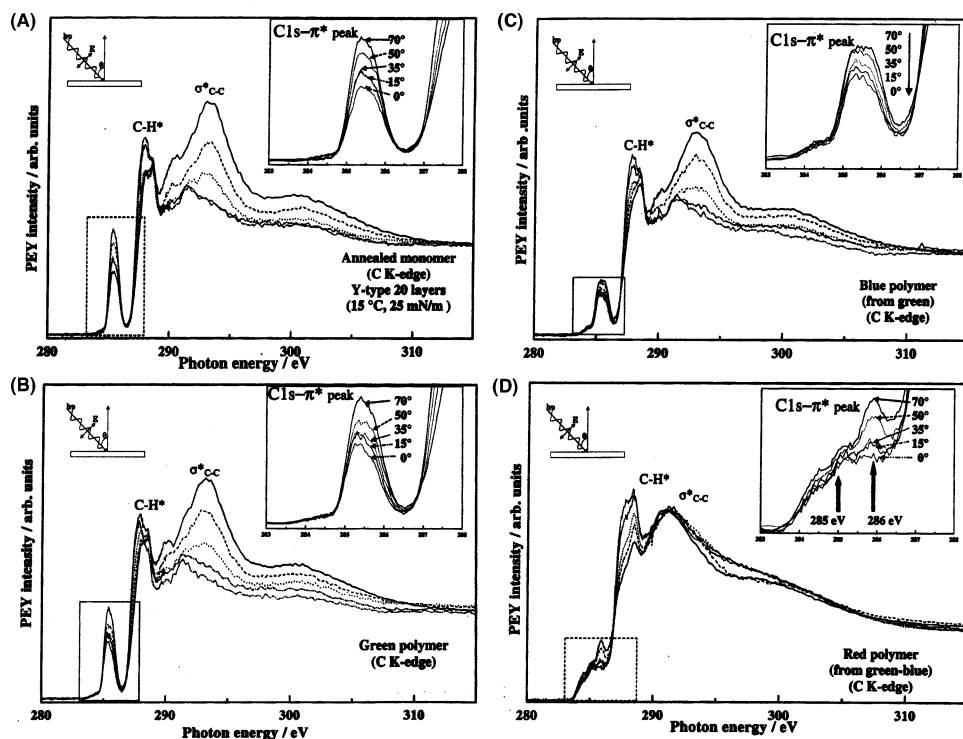


Figure 6. Dependence of the incident angles on the C K-edge polarized NEXAFS spectra for LB multilayers (20 layers, 25 mN/m, 15 °C) of CdDA[11–8]: (A) annealed monomer, (B) green polymer, (C) blue polymer, and (D) red polymer on NESA glass substrate.

Seki et al. showed the UPS spectra of evaporated and LB films of 10,12-tricasadiynoic acid and their cadmium salts before and after polymerization at the Xe I resonance line ($h\nu = 8.42$ eV).^{18–20} The ionization threshold energy (I_{th}) of the monomer was determined to be 7.0 eV (LB; 6.7 eV). After polymerization,

both the blue and the red films had similar spectra, with I_{th} values of 5.2 and 5.1 eV, respectively. These values are much smaller than that of the monomer. The 1.7 eV reductions in I_{th} are explained by the lower half of the energy correlation diagram on the left-hand side of Figure 5D. The π -electron states of the

diacetylene monomer are composed of a doubly degenerate bonding (π_1) and antibonding (π_2) combination of the π highest occupied molecular orbital (HOMO) of acetylene. Upon polymerization, the $2p_z$ orbital vertical to the molecular plane forms a delocalized π band, with the top (π_t) 1.7 eV higher than the HOMO of diacetylene. In the acetylenic form, the conformation for the blue film,⁴⁰ the $2p$ orbital in the molecular plane at each triple bond forms a localized π -bond (π_n). The known splitting between the π_1 - and π_2 -orbitals of diacetylene is 2.4 eV;⁴¹ thus, assuming a symmetric band, the total width of the π -band was estimated to be 5.8 eV. On the right-hand side of Figure 5D, the results of equivalent core MO calculations for acetylene, diacetylene, and a model molecule of diacetylene polymer $\text{CH}_2=\text{CH}-(\text{C}\equiv\text{C}-\text{C}=\text{C})_3-\text{H}$ are shown. The intensity of the transition to the upper π^* -state (π_4^*) for the monomer was determined to be much smaller than that to the lower π^* -state (π_3^*). The value is consistent with that of acetylene, which agrees with that reported for the same excitation energies (285.5 eV).⁴² These results enabled panel A in Figure 6 to be assigned to the transition to the π_3^* -state. The splitting of each peak is due to the difference in the effect of the core hole created between excitations from the inner and outer carbons of the $-\text{C}\equiv\text{C}-\text{C}\equiv\text{C}-$ unit.^{15,19,43} However, the splitting of $\text{C}1s-\pi^*$ transition peaks was not confirmed in the cadmium salt film in this study. Therefore, the inner and outer carbons of the diacetylene functional group in the LB film for diynic acid cadmium salt were determined to be almost equivalent. This was thought to be because molecular packing mainly affected hydrophobic chain-chain interactions (although the splitting of $\text{C}1s-\pi^*$ peaks was observed in the spectrum for metal-free acid film, later). The spectrum for the polymer of electric vector E of light vertical to the molecular plane shows two peaks, corresponding to excitations to π_b^* and π_t^* , whereas the spectrum for E in the molecular plane shows an intense peak corresponding to an excitation to the nonbonding orbital (π_n^*). Again, the small splitting in the lowest excitation is due to the site-dependent core-hole effect. The intensity of the transition to π_t^* is much smaller than those to π_b^* and π_n^* . These observations were in good agreement with the previous experimental observation of two peaks on NEXAFS spectra of evaporated films of 10,12-tricasadiynoic acid. Thus, the peaks at ~ 284.6 and 285.6 eV were assigned to the excitations to π_b^* and π_n^* , respectively. According to previous calculations, the $\text{C}1s-\pi^*$ peak for blue polymer LB films at 285.5 eV in this study was thought to correspond to the $\text{C}1s-\pi_b^*$ transition and the 285.0 eV peak in red polymer to the $\text{C}1s-\pi_n^*$ transition.

Panels A, B, C, and D in Figure 6 respectively show the NEXAFS spectra of annealed CdDA[11–8] monomer film, Poly-CdDA[11–8] green film obtained by UV irradiation from annealed CdDA[11–8] monomer film, and Poly-CdDA[11–8] blue and red films obtained by further UV irradiation to the greenish polymer films. The NEXAFS spectra shown in Figure 6A clearly depicts one difference in that there is a dependence on the incident angle for the $\text{C}1s$ to the π^* transition peak in comparison with that shown in Figure 5A. The spectra of annealed CdDA[11–8] monomer films, the peak at 285.5 eV, which was attributed to the π^* orbital of the functional groups, reached a maximum at the grazing incidence ($\theta = 70^\circ$) and was weakened at normal incidence. The very clear polarization dependence of the $\text{C}1s$ -to- π^* transition indicates highly ordered functional groups with an almost perpendicular orientation to the π^* orbital. The results of Figures 6B and 6C revealed that a dependence on the incident angle existed for the spectra of green and blue polymers. This indicates

that these polymers maintained a highly regular molecular orientation, and the difference between the molecular structure of blue films obtained is the formation of nonannealed monomer films and annealed monomer films via the greenish film. The characteristic change of the NEXAFS spectra is also displayed for the red films. Although the polarization dependence for the $\text{C}1s$ -to- $\sigma^*(\text{C}-\text{C})$ transition peaks disappeared, that for the $\text{C}1s$ -to- $\sigma^*(\text{C}-\text{H})$ transition peaks was maintained and the $\text{C}1s$ -to- π^* transition peak was split, shifting from 285.5 to 286.0 eV (possibly the $\text{C}1s-\pi_t^*$ transition) and 285.0 eV. Furthermore, the peak at 286.0 eV exhibited a dependence on polarization, whereas no dependence for that at 285.0 eV was observed. These two peaks on the diacetylene derivative red films in the higher- and lower-energy region are thought to correspond to the transition to the delocalized π_t^* band and the isolated π_n^* orbital in the triple bond, respectively. However, the splitting of these peaks was not consistent with results of the previous studies of LB films for 10,12-tricasadiynoic acid cadmium salt. This is thought to be because polymerization does not progress regularly, because of the formation of ineffective molecular packing for polymerization. Although the reason for the incomplete polymerization in LB multilayers has been previously suggested to be due to disordered molecular arrangement, the obstruction of progression of polymerization is now thought to be due to the formation of a highly order molecular orientation along the long molecular axis, which is clearly dependent on the polarization and lack of regularity of the polymerizable functional groups.

Figure 7 shows plots of the normalized 285.5 eV peak intensity versus the incident angle of the NEXAFS spectra. The comparison of the uniformity of alignments for the functional groups of several diacetylene and polydiacetylene films was conducted for the normalization of the $\text{C}1s$ -to- π^* transition peaks by an edge-jump inversion and a plot of these values. As these plots show, although the uniformity of alignment of the functional groups was slightly reformed upon UV irradiated photopolymerization of the nonannealed system (Figure 7, left-hand side), in the annealed system, the regularity of functional group arrangements formed by annealing declined with the polymerization reaction (Figure 7, right-hand side). The split $\text{C}1s$ -to- π^* transition peaks at 286.0 eV on red films from annealed monomer film, via green and blue films, increased the normalized intensity, compared with the blue film, because of the reorientation, together with the color phase transition, whereas the dependence on the incident angle of the 285.0 eV peaks disappeared for both red films. According to the aforementioned interpretation, the orientation of the π_t^* orbital in the red polymer film was more ordered than that of the π_b^* orbital in the blue film.

Photopolymerization of Multilayers for Metal-Free Diynic Acid Derivatives. In the π -A isotherm of DA[11–8] metal-free monolayers at 15°C , DA[11–8] monolayers formed expanded films with limiting areas of $\sim 39.5 \text{ \AA}^2$ on distilled water (pH 5.8). This finding was thought to be because CdDA[11–8] monolayers exhibited a relatively narrow distance between molecules, compared to that observed for metal-free DA[11–8]. This was due to the formation of a bivalent salt for the Cd^{2+} ion, whereas the carboxyl group of the DA[11–8] metal-free acid has a rigid diacetylene group in the center of molecule, which was not sufficiently dissociated at pH 5.8. Thus, DA[11–8] molecules formed expanded monolayers. (However, the formation of the stable condensed monolayer was not achieved at every pH without metal salt formation, because of the strong influence for the existence of rigid diacetylene

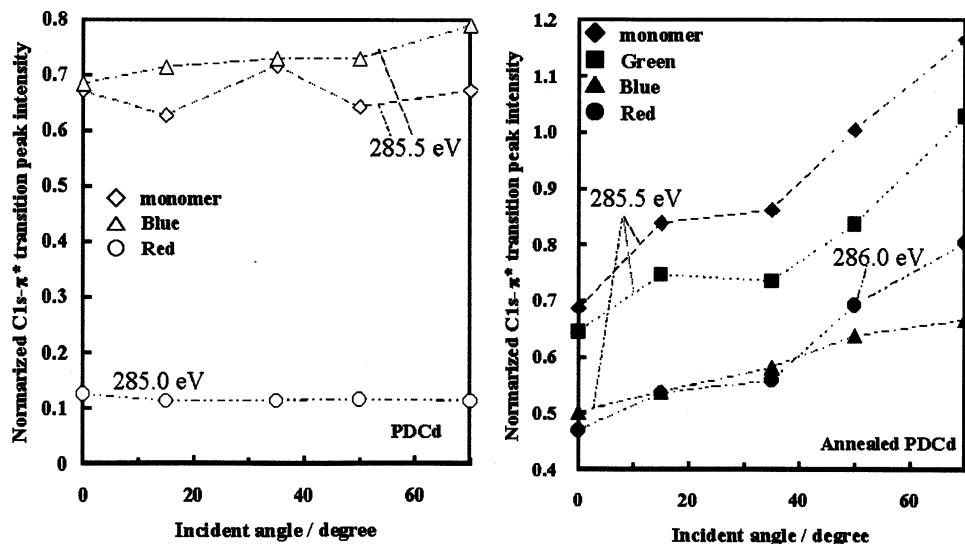


Figure 7. Plots of the normalized C1s- π^* transition peak intensity versus the incident angle.

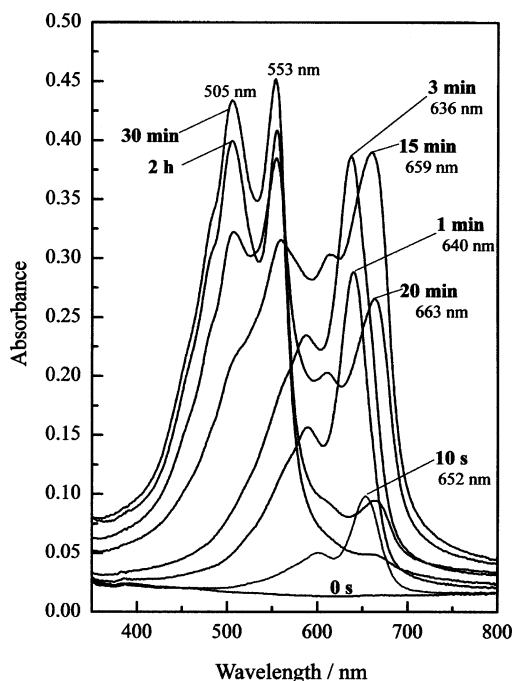


Figure 8. Visible absorption spectra for multilayers (20 layers, 11 mN/m, 15 °C) of DA[11-8] and their polymers on a quartz substrate.

groups in the center of molecule, although there is a slight dependence of the π -A isotherm for the DA[11-8], based on the change in the degree of dissociation of DA[11-8] free acid at the higher pH value.)

Figure 8 shows visible absorption spectra, illustrating the color change of DA[11-8] metal-free multilayers and their polymers upon photopolymerization. DA[11-8] multilayers were transferred by the horizontal lifting method at low surface pressure, because these molecules could not form stable monolayers on the water surface. Upon irradiation with UV light, blue-colored Poly-DA[11-8] rapidly formed in the transferred film. After 1 min of UV irradiation, the spectra indicated an absorption maximum at 640 nm, and this absorption band gradually shifted to the short wavelength side of the spectrum. The value of absorption intensity was remarkably higher than that of CdDA[11-8] LB film. The absorption band at \sim 550 nm indicated that the red color increased after 15 min of continuous UV irradiation, and the absorption band indicated that the blue

color ceased and shifted to the long-wavelength side of the spectrum. The absorption band in the blue region of the spectrum gradually attenuated and shifted toward the long-wavelength side of the spectrum. The absorption maximum was determined to be >660 nm after 20 min of irradiation. Ten minutes later, Poly-DA[11-8] completely changed to a red color film with an absorption maximum of 505 and 553 nm. The red color of these absorption bands maintained a strong intensity, without attenuation, even after 2 h of UV irradiation. However, the following areas require further investigation:

(1) The reason for an absorbance that is 3.5 times larger than that of the CdDA[11-8] LB film remains unclear.

(2) A structural characterization for the red polymer that maintained a strong visible spectra intensity over 2 h UV irradiation has yet to be accomplished.

(3) The cause of the gradual attenuation shift toward the longer-wavelength region of the absorption band in the blue region of the spectrum remains unidentified.

An analysis of the film structure and discussion of the interaction of the molecular packing are discussed in the following section.

Structural Estimation of DA[11-8] Films and Discussion of the Origin of the Color Phase Transition of Polydiacetylene. Figure 9 shows the out-of plane and in-plane XRD profiles of multilayers of DA[11-8] and their polymers. From these experiments, the layer structure and packing mode of the subcell for the side chain on the free acid multilayers were clearly exhibited. That is, the blue-red color phase transition in this system is observed to involve a very characteristic rearrangement of the side chains. The monomer film was determined to form a Y-type, multilayer, double-layered structure, because the out-of plane XRD pattern of monomer films exhibited a bilayer spacing of 45.0 Å. Although the deposition was performed by the horizontal lifting method, the film molecules were suggested to invert and form a piled bilayer structure for head-to-head and tail-to-tail forms, because of the unstable orientation of the hydrophilic groups upon exposure to the air. (According to the Petty's textbook, in the section on the XRD study of organized molecular films for fatty acid metal salt, there is co-recognition of the phenomena that the film molecules in multilayers transferred by a horizontal lifting method turned over and formed from single-layered (X-type) to the double-layered (Y-type) structure, among the investigators in this field. However, there is no report of direct observation

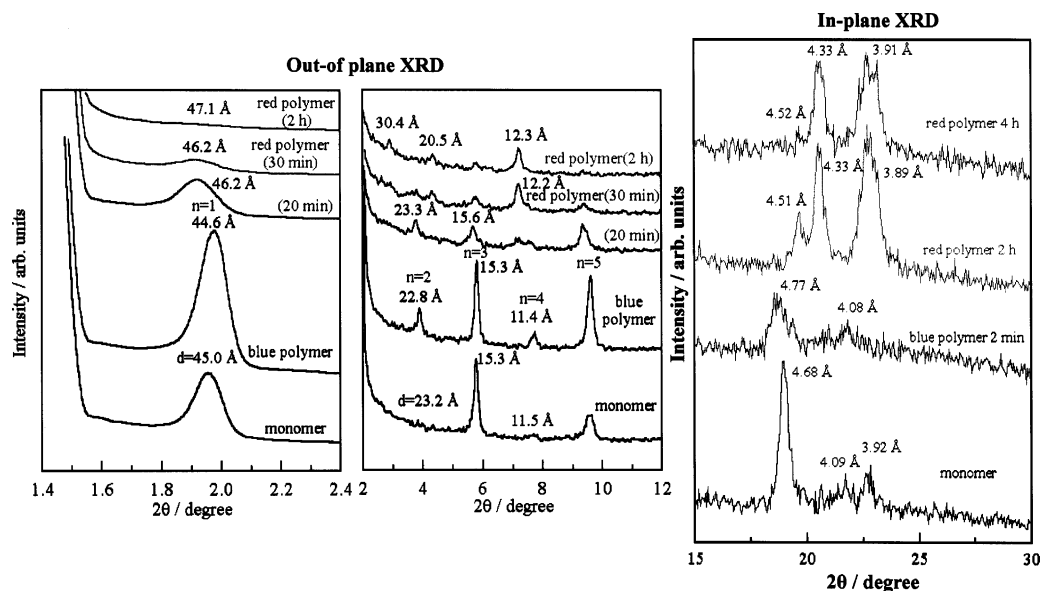


Figure 9. Out-of-plane and in-plane XRD profiles of multilayers (20 layers, 11 mN/m, 15 °C) of DA[11–8] and their polymers on a glass substrate.

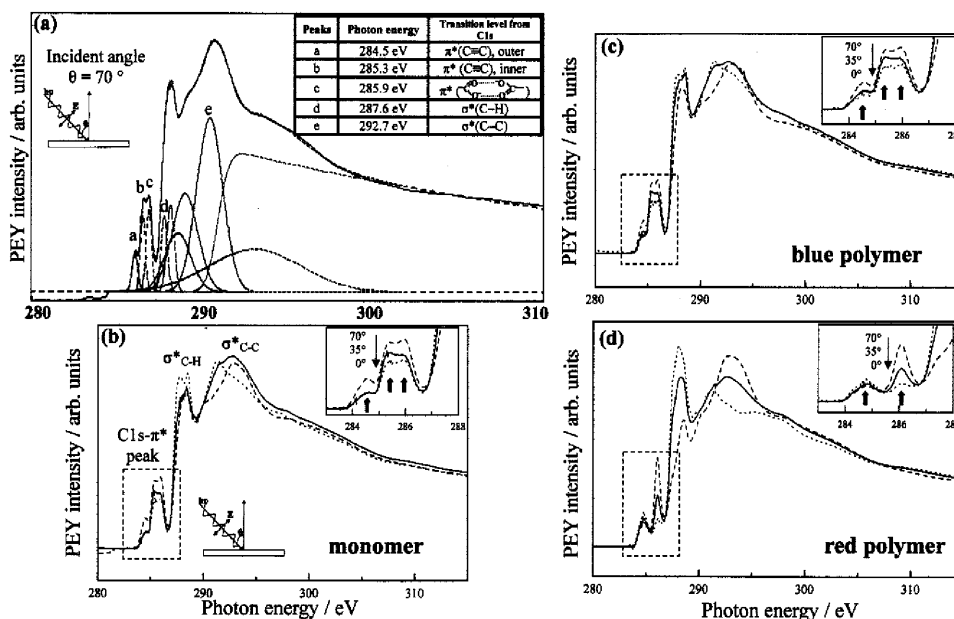


Figure 10. Curve fitting of the C K-edge NEXAFS spectra for the DA[11–8] multilayers (20 layers, 11 mN/m, 15 °C), and their assignments (inset), and incident angle dependence of NEXAFS spectra for (a) multilayers (20 layers, 11 mN/m, 15 °C) of DA[11–8] (B) monomer, (C) blue polymer, and (D) red polymer on NESA glass substrate.

of these mechanisms. The origin of this peculiar behavior is believed to be the unstable conformation of film molecules exposed hydrophilic group to the air, and it is an obvious fact of formation for the double-layered (Y-type) structure in the film, based on the conformation of a double-layered spacing in the XRD profile. If we must make a deduction regarding this phenomenon, the film molecules probably turned over at the moment of transfer, that is, just as the substrate surface separated from the subphase, although there is no positive proof, yet.) The two-dimensional lattice of the monomer film formed a quasi-hexagonal system with an in-plane spacing of 4.68 Å, indicating a small distortion and confirming the narrow spacing at 4.09 and 3.92 Å. After polymerization and formation of the blue polymer film, a layer structure developed, with higher XRD intensity. The in-plane lattice was distorted to an orthorhombic system with a spacing of 4.77 and 4.08 Å, and the polymerization progressed along the film plane. Furthermore, rearrangement of the side chains and change of the tilted angle of

molecules, in addition to the color phase transition from blue to red have been confirmed by XRD patterns. A distorted ordered two-dimensional lattice formed in the red polymer, exhibiting relatively narrow in-plane spacing, although the layer structure itself was declined. The color phase transition from blue to red, in which the in-plane orientation of the red polymer formed an ordered structure, differed from the trends seen for CdDA[11–8], in which the blue film formed an ordered structure. This tendency is thought to be due to the rearrangement of side chains with the color phase transition, which were dependent on the molecular packing and, thus, affected interactions in the film.

Figure 10 shows the curve-fitting analysis of the C K-edge NEXAFS spectra for the DA[11–8] multilayers and the dependence of the incident angle of NEXAFS spectra for multilayers of the DA[11–8] monomer, blue polymer, and red polymer. From the NEXAFS measurement, information on the change of the alignment for the conjugated backbone of

rearranged free acid multilayers with photopolymerization and color change transition could be acquired. In Figure 10A, the C K-edge NEXAFS spectra at the grazing incident angle ($\theta = 70^\circ$) of the DA[11–8] monomer multilayers were fitted using the Gaussian function. One of most distinctive features of this spectrum was the existence of three peaks at the lower-energy end of the spectrum. The peaks at 284.5 and 285.3 eV were assigned to the outer and inner carbon of diacetylene functional groups. The inequivalency of carbons for functional groups was determined to affect primarily the π – π interactions of polymerizable functional groups, which affected the molecular packing in the film.^{15,19,43} The molecular orientation of CdDA[11–8] monomers was controlled by the LB method, and molecular packing was mainly controlled by hydrocarbon-chain–hydrocarbon-chain interactions. The structure of the DA[11–8] monomer film could not be fully controlled by the procedure of formation for the monolayer on the water surface and the horizontal lifting method, because of factors including the incomplete dissociation of carboxyl group, the existence of a rigid diacetylene group in the center of the molecule, the formation of an expanded monolayer, the lower collapsed surface pressure of the monolayer, and the inversion of molecules in transferred films. Consequently, DA[11–8] molecules in the film were rearranged and packed by π – π interactions of functional groups, such as three-dimensional crystal growths.

The visible absorption spectra revealed that the peak intensity, which was 3.5 times greater than that of the CdDA[11–8], was based on the formation of a profitable packing of polymerization for metal-free acid films and the resultant conversion to a polymer of higher value than that of the cadmium salt. The shift to the longer-wavelength side of the spectrum, coupled with attenuation of the blue absorption band, implies an incomplete progression of polymerization in a short time. That is, the polymerization in the crystalline-like structure differed entirely from the topochemical reaction. Moreover, the formation of higher-molecular-weight polymers requires a certain amount of time and the progression of polymerization to the blue polymer with a higher degree of polymerization and color phase transition to the red polymer occurred simultaneously.

The peak at 285.9 eV represented the $C1s-\pi^*(C=O)$ transition of the carboxyl group for the DA[11–8] anion dimer ($-COO^- \cdots -OOC-$), because this peak was only slightly shifted upon polymerization or color phase transition; a shift in this region was not observed in previous studies that used evaporated diynoic acid derivative films or LB films of the cadmium salts. Although these three peaks exhibited a dependence on the incident angle, $C1s-\sigma^*(C-H)$ and $C1s-\sigma^*(C-C)$ peaks from the monomer and blue polymer films did not exhibit dependence on the polarization incident soft X-ray, because of the disordering of the molecular orientation. However, in the red film, the dependence on the incident angle of the $C1s-\sigma^*(C-H)$ and $C1s-\sigma^*(C-C)$ transition peaks was confirmed and the $C1s-\pi^*$ transition peaks of the outer and inner carbons of the diacetylene group shifted to ~ 285.0 eV. The peak at 285.0 eV was thought to be a typical transition for the red polymer film, which was also observed in the cadmium salt film. It is well-known that the diacetylene red polymer film is fluorescent; this fluorescence is believed to be a result of the energy-level transition.

Until now, the color phase transition of polydiacetylene from the blue film to the red film has been interpreted in many ways. One such explanation is that the molecular orientation of the red film was disordered, whereas others disagreed. The present

investigation proposes that the change in the orientation of the conjugated backbone, not the arrangement of the side chain, induced the color phase transition from the blue polymer to the red polymer. Rather, the side-chain arrangement was varied by the change of the conjugated backbone and the color phase transition. Moreover, the differing views of the color phase transitions of polydiacetylene was due to the formation of the film structure of the diacetylene monomer, in which the molecular packing of the organized molecular film was controlled by the chain–chain interaction of the side chains or the π – π interactions of the polymerizable functional group. If two-dimensional packing of the films was controlled by hydrocarbon-chain–hydrocarbon-chain interactions, as in the LB films of cadmium salt long-chain diynoic acids or the self-assembled monolayer, the inner and outer carbons of the diacetylene groups would be equivalent, and the orientation of the side chains on the red polymer film would be disordered. If however, the molecular packing of the films was controlled by π – π interactions of the functional group as in the LB films from metal-free long-chain diynoic acid, evaporated films, and crystals, the NEXAFS spectra for the $C1s-\pi^*$ transition peaks would be split, because of the inequivalence of the inner and outer carbons of the diacetylene groups, and the orientation of the side chains on the red polymer may exhibit rearrangement of ordering. The degree of order or disorder for side chains on the red film are thought to be controlled by the regularity of the molecular orientation for the monomer film, based on the deposition procedure. The rearrangement of the conjugated backbone indicated a shift of the $C1s-\pi^*$ transition peaks in the NEXAFS spectra to ~ 285.0 eV, which caused a color phase transition from the blue polymer film to the red polymer film. This rearrangement of the conjugated backbone with the color phase transition was suggested to shorten the effective conjugated length, because of the distortion and twist of the conjugated system. The results of in-plane XRD confirmed relatively shorter two-dimensional lattice spacing.

In the comparison with cadmium salt, almost the same changes in the arrangement for the conjugated polymer backbone (main chain) of CdDA film and DA film to the UV irradiation are observed. However, there is a remarkable difference in the arrangement of the side chains between both films. That is, if highly ordered side-chain orientation is formed using a method of organized molecular films (ex, method of monolayer on the water surface, LB method, and other transferring methods), disordering of the side-chain arrangement results, together with rearrangement of the conjugated backbone by color phase transition. While, if highly ordered side-chain orientation is not formed via a method of organized molecular films, ordering of the side-chain arrangement results, together with rearrangement of the conjugated backbone.

4. Conclusions

The monolayer behavior on the water surface and the effect of molecular arrangements with annealing upon photopolymerization in diynoic acid cadmium salt transferred films were investigated. The formation of a greenish polymer film with an extended conjugate system was determined to be related to the film structure. The angular dependence of the incident X-ray on the near-edge X-ray absorption fine structure (NEXAFS) spectra for the organized molecular films of long-chain diynoic acid derivatives on solids elucidated the orientation of the functional groups after annealing and photopolymerization. The dependence on the incident angle of the $C1s-\pi^*$ transition peaks for the annealed transferred film with extended conjugate

systems was confirmed by C K-edge polarized NEXAFS spectroscopy. However, these dependencies were not observed on the nonannealed multilayer films.

Furthermore, metal-free 10,12-pentacosadiynic acid films were also examined after photopolymerization and their structure was elucidated. The red-colored polymer film in this system formed a highly ordered molecular orientation with a shift of the NEXAFS spectra C1s- π^* transition peaks. The regularity of the molecular arrangement for monomer and blue polymer films could not be confirmed.

The color phase transition of diacetylene derivatives with photopolymerization caused rearrangement of the conjugated backbone, supported by a shift of the C1s- π^* band on the NEXAFS spectra; the reorientation of the side chains was affected by the structural change of the conjugated system.

Acknowledgment. The authors greatly appreciate Dr. Kenta Amemiya (Tokyo University) for his assistance with the NEXAFS measurements and helpful discussions. The authors thank the Japan Society for Promotion of Science for the postdoctoral fellowship to A.F. This work was performed under the approval of the Photon Factory Program Advisory Committee (Proposal No. 2000G282 and 2002G288).

References and Notes

- (1) Wegner, G. Z. *Naturforsch., B: Anorg. Chem., Org. Chem., Biochem., Biophys. Biol.* **1969**, *24b*, 824. Wegner, G. In *Molecular Metals*; Hatfeld, W. E., Ed.; Plenum: New York, 1979, p 209.
- (2) Tieke, B.; Wegner, G.; Naegele, D.; Ringsdorf, H. *Angew. Chem., Int. Ed.* **1976**, *15*, 764.
- (3) Batchelder, D. N.; Evans, S. D.; Freeman, T. L.; Häussling, L.; Ringsdorf, H.; Worf, H. *J. Am. Chem. Soc.* **1994**, *116*, 1050.
- (4) Kanetake, T.; Tokura, Y.; Koba, T. *Solid State Commun.* **1985**, *56*, 803.
- (5) Sauert, C.; Herman, J. P.; Fer, R.; Predieere, F.; Ducing, J.; Baughman, R. H.; Chance, R. R. *Phys. Rev. Lett.* **1976**, *36*, 956.
- (6) Kasai, H.; Tanaka, H.; Okada, S.; Oikawa, H. *Chem. Lett.* **2002**, 696.
- (7) Tieke, B.; Lieser, G. *J. Colloid. Interface Sci.* **1982**, *88*, 471.
- (8) Day, D.; Land, J. B. *Macromolecules* **1980**, *13*, 1478.
- (9) Bloor, D.; Chance, R. R., Eds. *Polydiacetylenes*; Martinus Nijhoff: Dordrecht, The Netherlands, 1985.
- (10) Schott, M.; Wegner, G. In *Nonlinear Optical Properties of Organic Molecules and Crystals*; Chamla, D. S., Zyss, J., Eds.; Academic Press: Orlando, FL, 1987.
- (11) Kim, T.; Crooks, R. M.; Tsen, M.; Sun, L. *J. Am. Chem. Soc.* **1995**, *117*, 3963.
- (12) Mowery, M. D.; Kopta, S.; Ogletree, D. F.; Salmeron, M.; Evans, C. E. *Langmuir* **1999**, *15*, 5118.
- (13) Fukuda, K.; Shibasaki, Y.; Nakahara, H. *Thin Solid Films* **1983**, *99*, 87.
- (14) Fukuda, K.; Shibasaki, Y.; Nakahara, H. *Thin Solid Films* **1985**, *133*, 39.
- (15) Stöhr, J. *NEXAFS Spectroscopy*; Springer: Berlin, 1992.
- (16) Outka, D. A.; Stöhr, J.; Rabe, J. P.; Swalen, J. *J. Chem. Phys.* **1988**, *88*, 4076.
- (17) Nakahara, H.; Fukuda, K.; Seki, K.; Asada, S.; Inokuchi, H. *Chem. Phys.* **1987**, *118*, 123.
- (18) Fukuda, K.; Shibasaki, Y.; Nakahara, H. *Thin Solid Films* **1988**, *160*, 43.
- (19) Seki, K.; Morisada, I.; Tanaka, K.; Edamatsu, M.; Yosiki, M.; Tanaka, Y.; Yokoyama, T.; Ohta, T.; Asada, S.; Inokuchi, H.; Nakahara, H.; Fukuda, K. *Thin Solid Films* **1989**, *179*, 15.
- (20) Seki, K.; Morisada, I.; Edamatsu, K.; Tanaka, H.; Yanagi, H.; Yokoyama, T.; Ohta, T. *Phys. Scr.* **1990**, *41* (1), 173.
- (21) Seki, K.; Yokoyama, T.; Ohta, T.; Nakahara, H.; Fukuda, K. *Mol. Cryst. Liq. Cryst.* **1992**, *218*, 609.
- (22) Evans, C. E.; Smith, A. C.; Burnett, D. J.; Marsh, A. L.; Fisher, D. A.; Gland, J. L. *J. Phys. Chem. B* **2002**, *106*, 9036.
- (23) Gains, G. L., Jr. *Insoluble Monolayers at Liquid Gas Interface*; Wiley: New York, 1966.
- (24) Fukuda, K.; Nakahara, H.; Kato, T. *J. Colloid Interface Sci.* **1976**, *54*, 430.
- (25) Fujimori, A.; Araki, T.; Nakahara, H.; Ito, E.; Hara, M.; Ishii, H.; Ouchi, Y.; Seki, K. *Langmuir* **2002**, *18*, 1437.
- (26) Fujimori, A.; Araki, T.; Nakahara, H.; Ito, E.; Hara, M.; Ishii, H.; Ouchi, Y.; Seki, K. *Chem. Phys. Lett.* **2001**, *349*, 6.
- (27) Kojio, K.; Takahara, A.; Omote, K.; Kajiyama, T. *Langmuir* **2000**, *16*, 3932.
- (28) Amemiya, K.; Kitajima, Y.; Ohta, T.; Ito, K. *J. Synchrotron Rad.* **1996**, *3*, 282.
- (29) Kitajima, Y.; Yokoyama, Y.; Amemiya, K.; Tsukabayashi, H.; Ohta, T.; Ito, K. *J. Elec. Spectrosc. Relat. Phenom.* **1999**, *927*, 101.
- (30) Seki, K.; Mitsumoto, R.; Ito, E.; Araki, T.; Sakurai, Y.; Yoshimura, D.; Ishii, H.; Ouchi, Y.; Miyamae, T.; Narita, T.; Nishimura, S.; Takata, Y.; Yokoyama, T.; Ohta, T.; Suganuma, S.; Okino, F.; Touhara, H. *Mol. Cryst. Liq. Cryst.* **2001**, *355*, 247.
- (31) Tieke, B.; Wegner, G. *Topics in Surface Chemistry*; Kay, E., Bagus, P. S., Eds.; Plenum: New York, 1979; p 121.
- (32) Kuhn, H. *Fortschr. Chem. Org. Naturst.* **1959**, *17*, 404.
- (33) Fujimori, A.; Saitoh, H.; Shibasaki, Y. *J. Polym. Sci. Polym. Chem. Ed.* **1999**, *37*, 3845.
- (34) Tokura, Y.; Kanetake, T.; Ishikawa, K.; Koba, T. *Synth. Met.* **1987**, *17*, 407 and references therein.
- (35) Eckhardt, D. S.; Boudreaux, D. S.; Chance, R. R. *J. Phys. Chem.* **1986**, *85*, 4116.
- (36) Stöhr, J.; Outka, D. A. *Am. Phys. Soc.* **1987**, *36*, 7891.
- (37) Outka, D. A.; Stöhr, J.; Madix, R. J.; Rotermund, H. H.; Hermesmeier, B.; Solomon, J. *Surf. Sci.* **1987**, *53*, 185.
- (38) Ouchi, Y.; Mori, I.; Seki, M.; Ito, E.; Araki, T.; Ishii, H.; Seki, K.; Kudo, K. *Physica B* **1995**, *208/209*, 407.
- (39) Horsly, J. A.; Stöhr, J.; Hitchcock, A. P.; Newbury, D. C.; Johnson, A. L.; Sette, F. *J. Chem. Phys.* **1985**, *83*, 6099.
- (40) Kobeld, D.; Paulis, E. F. *Acta Crystallogr., Sect. B: Struct. Crystallogr. Cryst. Chem.* **1973**, *B30*, 232.
- (41) Baker, C.; Turner, D. W. *J. Chem. Soc. Chem. Commun.* **1967**, 797. Heilbronner, E.; Jones, T. B.; Maier, J. P. *Helv. Chim. Acta* **1977**, *60*, 1697.
- (42) Outka, D. A.; Stöhr, J. In *Chemistry and Physics of Solid Surfaces VII*; Vanselow, R.; Howe, R.F., Eds.; Springer Series in Surface Sciences 10; Springer-Verlag: Berlin, New York, 1988.
- (43) Naves de Brito, A.; Svensson, S.; Correia, N.; Keane, M. P.; Agren, H.; Sairanen, O.-P.; Kivimarki, A.; Aksela, S. *J. Electron. Spectrosc. Relat. Phenom.* **1992**, *59*, 293.